

SUPPRESSION OF ASPHALTENE ADSORPTION IN POROUS MEDIA

Vineet Venkatanarayanan

A thesis

submitted in partial fulfilment of the
requirements for the degree of

Master of Science in Chemical Engineering

University of Washington

2017

Committee:

John C. Berg

Qiuming Yu

Program Authorized to Offer Degree:

Chemical Engineering

©Copyright 2017

Vineet Venkatanarayanan

University of Washington

ABSTRACT

SUPPRESSION OF ASPHALTENE ADSORPTION IN POROUS MEDIA

Vineet Venkatanarayanan

Chair of the Supervisory Committee:

Dr. John C. Berg

Rehnberg Professor of Chemical Engineering

Department of Chemical Engineering

This work seeks to investigate the adsorption/deposition of asphaltene clusters and nanoaggregates in a porous medium, under flow conditions and at high pressures. It also explores the strategies to reduce or prevent the adsorption/deposition. Asphaltenes are highly aromatic and heavy fractions present in crude oil. Their adsorption or deposition causes problems during production due to clogging of the pore structure of the rock as well as subsequently fouling downstream piping and fittings. The porous medium used in this study is 140 mesh silica (100 micron) packed into an HPLC (high performance liquid chromatograph) column through which dilute solutions of asphaltenes in a weak solvent (toluene and tetradecane 50 % by wt.) are pumped. Langmuir isotherms fit well to the adsorption results. Saturation asphaltene adsorption (Γ_{\max}) of about 1250 mg/m² is obtained for silica particles. To reduce or prevent such deposition, silica surface is modified using HTAB (hexadecyl trimethylammonium bromide), HMDS (Hexamethyldisiloxane) and OTS (Octadecyltrichlorosilane) to form a protective layer. Subsequent HPLC studies indicate that the saturation asphaltene adsorption on the treated silica has been reduced to 909.10 mg/m², 833.33 mg/m² and 588.23 mg/m² respectively.

To investigate the effects of adsorption/deposition on the porosity of the silica column, dilute solution of a high molecular weight asphaltene mimic, SEPTON 4099, in a similar solvent is pumped through the column under high pressure. Adsorption/deposition is monitored by changes in the pressure required to sustain a given flow rate, which is analyzed to give the resulting change in bed porosity, as deduced using Ergun analysis. A layer of thickness up to 3.6 μm is found to develop over a period of 60 hours. To reduce or prevent such deposition, the silica is pre-treated with HTAB to form a protective layer. Subsequent HPLC studies indicate that the polymer adsorption on the treated silica has been reduced to less than 50%.

1. INTRODUCTION

Asphaltene is the primary unresolved component of crude oil [1]. It consists of a highly aromatic core with a few aliphatic chains protruding out of the core. Along with the C and H atoms the asphaltenes also constitute of many different functional groups containing heteroatoms such as S, N, O, F and a few metals like Nickel and Vanadium which add to its polar nature [2]. A few studies indicate that asphaltene molecules contain primarily one polycyclic aromatic hydrocarbon ring (PAH) at the core with aliphatic chains surrounding the island structure [3], while other studies indicate multiple PAHs as the core of the asphaltene molecule [4]. The high aromaticity leads to a strong $\pi - \pi$ interaction which in turn leads to aggregation of the molecules. The difficulty in disaggregating an aggregated asphaltene molecule is the primary reason for conflicting studies [5]. The Yen-Mullins model is one of the best models that explain the aggregation of asphaltenes [6].

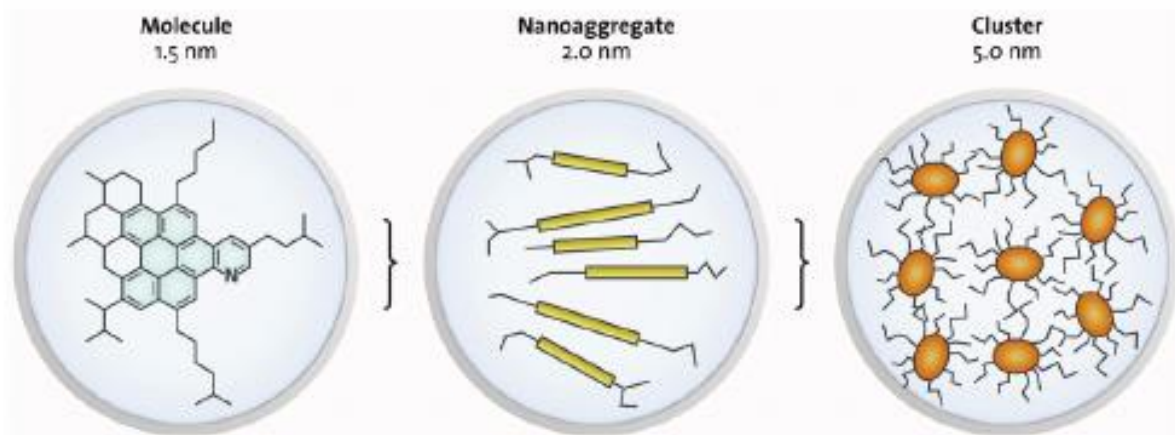


Fig 1: Yen – Mullins Model

Asphaltenes are the primary source of a number of economic problems that occur during the extraction, transportation and refining of the crude oil [7]. The nature and behavior of asphaltenes in crude oil is highly complex. It depends on various factors such as temperature, pressure and composition of the crude oil. During the extraction of crude oil, pressure and temperature decreases, this causes the asphaltenes to phase separate and

precipitate [8]. Various problems arise because of destabilized asphaltene such as clogging of capillaries in the reservoirs and well bores, change in wettability of reservoir – changes from water wet to oil wet which creates problems during extraction, formation of oil-water emulsions, adsorption onto equipment in the downstream refining processes, poisoning of catalyst, sedimentation during oil storage etc. [9]

Several studies confirm that the key elements of asphaltene adsorption, with regard to asphaltene selectivity, are the type and number of heteroatoms, types of functional group, aromaticity, size of the core, number and length of cleaved alkyl side, acid-base characteristics and amount of resinous material. There is a common consensus that the adsorption of asphaltenes is irreversible [10]. Prevention of asphaltene adsorption is of prime importance mainly due to the economic benefits involved [11].

Modifying silica substrates from a hydrophilic surface to hydrophobic surface has proven to be an effective way to reduce the adsorption of asphaltenes. Hannisdal et al. studied the effect of asphaltene adsorption by varying the wettability of silica particles. They modified the silica particles using 2-methacryloxypropyl trimethoxysilane, polydimethyl siloxane and dimethyl dichlorosilane [12]. The authors visually determined that the hydrophobic silica adsorbed less than hydrophilic silica particles. Their results were in agreement with the near-infrared spectroscopy measurements wherein they monitored the stretching vibration of the methylene groups, which gave the relative amount of hydrocarbon content on the silica surface. Their results led them to conclude that the adsorption of asphaltenes reduced as the hydrophobicity of the silica particles increased. Dudášová et al. studied asphaltene adsorption on hydrophilic and hydrophobic silica surfaces using UV-Vis spectroscopy [13]. The amount of asphaltene adsorbed was calculated from the difference in concentration of the asphaltene solution before and after the experiment. Their results showed that the adsorbed asphaltene concentration reduced from about 2.43 mg/m² to 0.52 mg/m² i.e.

the thickness of the adsorbed layer reduced from 2.05 nm to 0.43 nm (assuming a density of 1.2 gm/cc) for a hydrophobic surface.

The above studies concluded the effect of hydrophobicity on adsorption by studying only a few discrete surfaces. In order to firmly establish the role of hydrophobicity, Salomon Turgman-Cohen et al., varied the surface energy of silica particles systematically [14,15]. They studied the effect of asphaltene adsorption on Self-Assembled Monolayers (SAMs) of aliphatic and aromatic trichlorosilanes. In the first of a two-part study, SAMs of mixed aromatic and aliphatic trichlorosilanes were used to study adsorption. Spectroscopic ellipsometry was used to measure the thickness of the adsorbed layer and it was seen that the aromaticity of the SAMs played no role in asphaltene adsorption. In the second study the number of carbon atoms in the alkyl chain of the alkyltrichlorosilanes was increased systematically from 4 to 18. It was seen that the thickness of the adsorbed layer (determined through spectroscopic ellipsometry) remained constant at about 2 nm until the carbon chain length was increased to 18 at which point the adsorbed layer thickness drop to less than 1 nm. Their results led them to conclude that the hydrophobicity of silica substrates played no role in reducing the asphaltene adsorption, instead the ability of the silanes to shield the hydroxyl groups on the silica surface from interacting with the polar asphaltene molecules was the reason for reduced adsorption.

Two non-conforming studies exist that deny the role of a hydrophobic surface on reduced adsorption. Zahabi et al., studied the adsorption of pitch material from toluene solutions and reported that the hydrophobic and hydrophilic silica surface adsorbed in similar amounts [16]. In another case, the saturation limit of asphaltene adsorption was reported higher in case of hydrophobic silica (3.68 mg/m²) than hydrophilic silica (3.18 mg/m²) [17].

Asphaltenes adsorb on different surfaces as molecules or aggregates of different sizes [18]. The Yen-Mullins model (seen in Fig. 1) defines structures in the 1-2 nm range as molecules, 2-5 nm range as nanoaggregates and any bigger particulate is termed as clusters [6]. The amount of asphaltene adsorbed and the thickness of the adsorbed layer strongly depends on the solvent used for the study. This is because the asphaltenes dissolve as individual molecules in the strong solvents and as aggregates of increasing sizes as the solvent quality decreases [19,20]. For example, the studies conducted using strong asphaltene solvents such as toluene at low to moderate concentrations, show an adsorption of about 2-4 mg/m² (1.66 – 3.33 nm, assuming a density of 1.2 gm/cc) [21]. If the average size of an asphaltene molecule is assumed to be about 1.5 nm it can be argued that the asphaltenes in the above mentioned studies adsorbed as single or multiple layers of individual molecules. Very few studies exist that study the adsorption of asphaltenes using weak solvents. To have a thorough understanding of the effectiveness of silanes to reduce asphaltene adsorption, it is important to carry out experiments using solvents in which asphaltenes are dissolved in the form of nanoaggregates or clusters. It is also essential to conduct such experiments under flow conditions at high pressures. The following study covers all these major aspects.

In this study we have examined the effect of surface modification of silica particles with HTAB, OTS and HMDS on adsorption of asphaltenes under flow conditions using a weak solvent (toluene and tetradecane 50:50% by wt.). The weak solvents helped dissolve the asphaltene in its cluster form. In each case, the modification produced a hydrophobic silica surface altering the interaction between the asphaltene clusters and the silica particles. The adsorption of asphaltenes was measured by monitoring the UV-Vis absorbance of the effluent from the silica column. Appropriate isotherms were developed using the same. We further tried to investigate the effect of multilayer adsorption on the porosity of silica column by monitoring the pressure drop. As the asphaltenes failed to form a thick enough layer to cause

a change in pressure drop, we shifted to a high molecular weight asphaltene mimic (SEPTON 4099). Only one type of surface modification, using HTAB, was studied in this case. The size of asphaltenes and polymer clusters were determined by SEM imaging.

2. MATERIALS AND METHODS

2.1. Materials

Silica glass beads (140 mesh size, average diameter 100 μm) were obtained from Alibaba.com, a micrograph of the particles is shown in Fig. 2. SEPTON 4099 was obtained from Kuraray Co., Ltd (Houston, TX). The asphaltenes used here was extracted from Kuwaiti crude oil produced from the Marrat formation. Hexadecyltrimethylammonium bromide (HTAB) and HMDS (Hexamethyldisiloxane) were purchased from Sigma Aldrich (St. Louis, MO). Octadecyltrichlorosilane (OTS) was obtained from Gelest Inc. (Morrisville, PA).

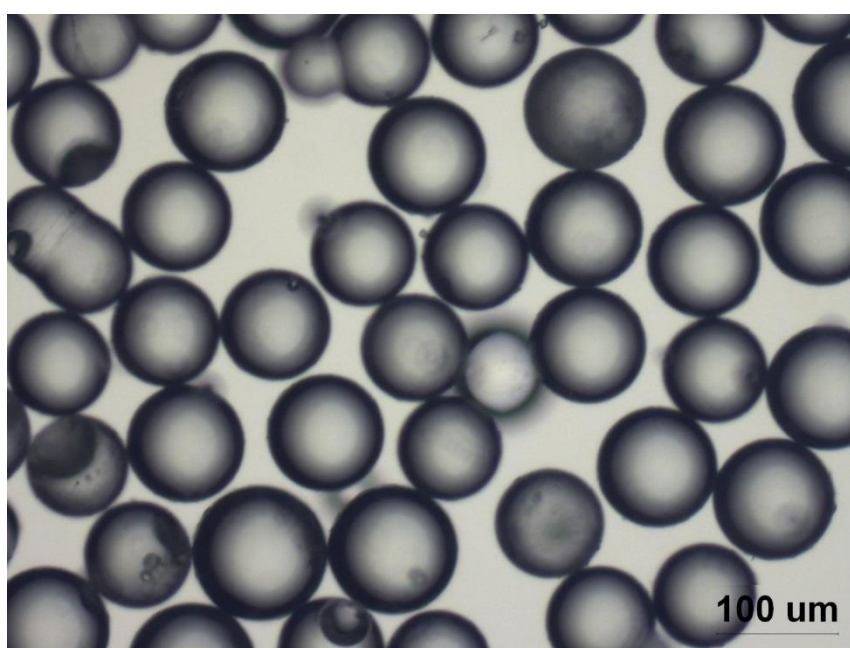


Fig 2: Micrograph of silica particles

2.2. Sample Preparation

2.2.1. Asphaltene solution preparation:

0.1, 0.2 and 0.4 wt.% (0.8, 1.6, 3.2 gm/lit respectively) asphaltene solutions were used to perform the flooding experiments. The solvent used was toluene and tetradecane 50% by wt. Equal weights of toluene and tetradecane were mixed in a clean glass beaker following which asphaltene was added and the sealed beaker was stirred overnight at room temperature until all the asphaltene aggregates were completely dissolved in the solvent.

2.2.2. SEPTON 4099 solution preparation:

0.5 wt.% (4 gm/lit) polymer solution was used to perform the flooding experiments. The solvent used was toluene and tetradecane 50% by wt. Equal weights of toluene and tetradecane were mixed in a clean glass beaker following which the polymer was added and the sealed beaker was stirred overnight at room temperature until all the polymer aggregates were completely dissolved in the solvent.

2.2.3. Silica surface modification with HTAB:

About 8 gm of silica particles were introduced in a clean glass beaker containing 100 ml DI water. 0.0364 gm of HTAB was added to the beaker, to make a surfactant solution at its critical micelle concentration. The sealed beaker was stirred at constant intervals for a period of 24 hours. The silica particles with adsorbed surfactant molecules were filtered and oven dried at 60 °C for a period of 5 hours.

2.2.4. Silica surface modification using OTS:

A 1% v/v solution of OTS in isopropyl alcohol was prepared in advance and allowed 60 min for hydrolysis of the silane while maintaining the pH at 4.5. The silica was then introduced in the solution and stirred for 90 min for complete reaction of the silane with the surface. The silica particles were then filtered out and oven dried at 80 °C for 5 hours.

2.2.5. Silica surface modification using HMDS:

Silica particles were completely immersed in HMDS in a clean glass beaker. The beaker was kept slightly ajar in an oven at 70 °C overnight. No filtration was required.

2.3.Experimental Setup

Figure 3 shows a schematic of the core flooding experimental setup. The setup is designed to study the asphaltene adsorption and deposition under dynamic conditions by measuring the pressure drop across the column and the UV-Vis absorption of the effluent. The apparatus is composed of the following:

An inlet solution reservoir connected to a high – pressure positive displacement pump that can pump liquid at a constant flow rate, a core holder than can be packed with a choice of silica, a differential pressure transducer that is connected to either ends of the core holder, a back pressure regulator which is used to regulate the pore pressure inside the core holder and finally an inline UV-Vis spectrometer that can measure the absorbance of the solution exiting the core holder as a function of time.

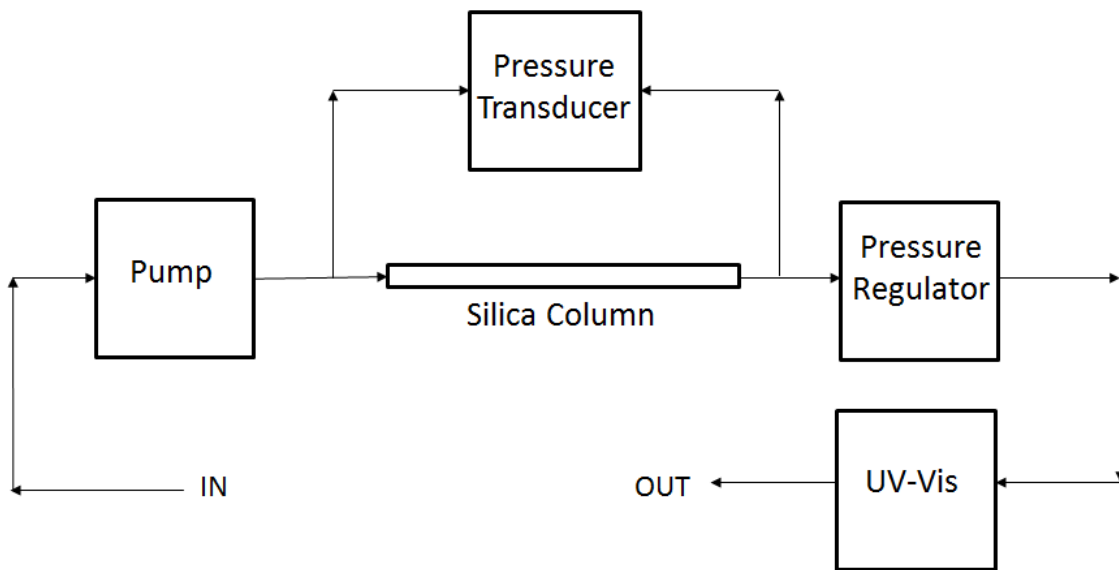


Fig 3: Schematic of the Core Flooding System

The core holder is a stainless steel column of length 4” and an inner diameter of ¼”. The column is filled with silica and is packed using fiber wool on either ends to entrain the particles. The back pressure regulator is pumped to a high pressure using an inert gas such as nitrogen. The back pressure regulator maintains the pressure inside the column and helps dissolve all the air molecules by increasing the air solubility of the hydrocarbon solvent from 0.001 mole fraction at atmospheric pressure to 0.011 mole fraction at 200 PSI.

2.4.UV – Vis Absorbance of Asphaltenes

Four asphaltene solutions of concentrations 0.025, 0.05, 0.075 and 0.1 wt.% were made following the procedure described above to obtain an absorbance versus concentration calibration curve. The absorbance measurements were made using a 1 mm quartz cuvette in Agilent Technologies' Cary 60 UV-Vis absorbance spectrometer. Figure 4 shows the calibration curves obtained for wavelengths 300, 400, 500 and 600 nm. The wavelength chosen for future analysis was 600 nm. Indeed, we have checked the variation of absorbance as a function of time and it did not show any noticeable change even after 24 hrs. of standing.

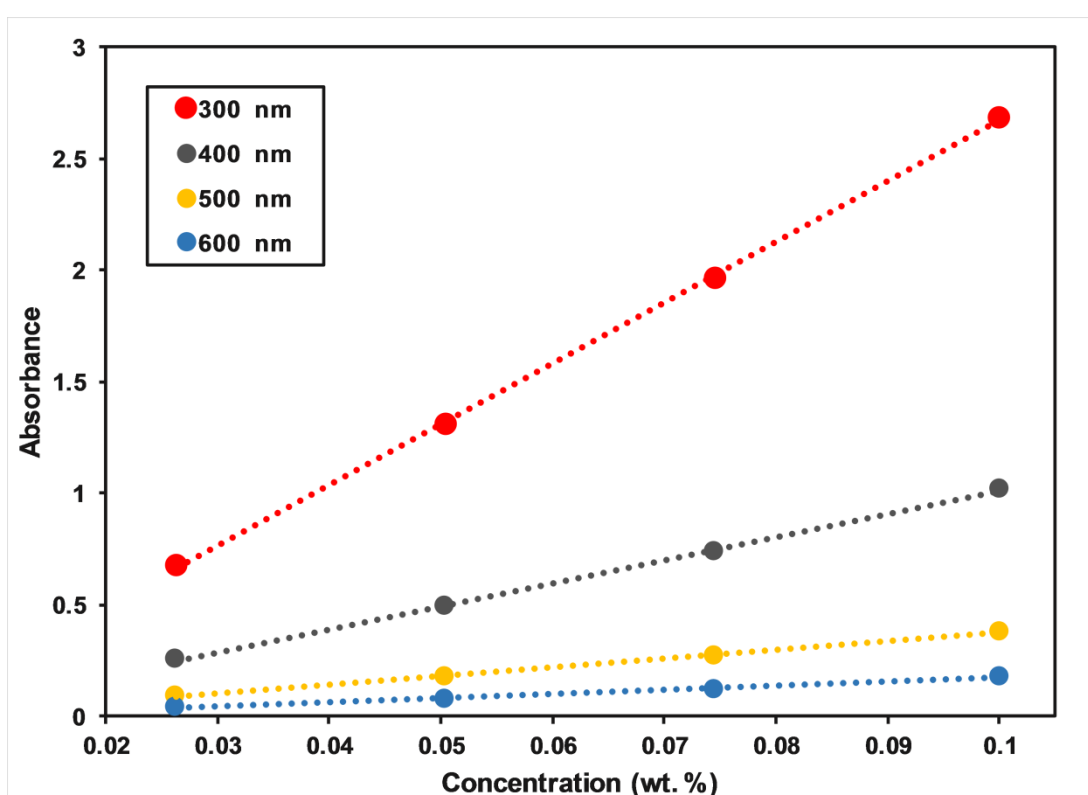


Fig 4: UV – Vis calibration curve of asphaltenes in toluene and tetradecane 50% by weight at 22 °C

2.5.Experimental Procedure

All the experiments were carried out at room temperature (22 °C). Before the start of each experiment, after packing the column with the choice of silica, pure solvent was pumped through the entire system to get rid of the trapped air bubbles, to wet the entire surface and get a blank reading for the absorbance spectrometer.

Experiment I(A) – In this experiment the core holder was packed with silica particles which were oven heated at 150 °C for 24 hours to remove all the moisture from its surface. Gonzalez et al., studied the effect of a thin moisture film on the adsorption of asphaltenes by systematically increasing the relative humidity of the system. Their findings show that the highest asphaltene adsorption takes place in the absence of a water film and decreases linearly as the thickness of the adsorbed surface moisture increases [22]. This makes the drying step extremely important. The asphaltene solutions were pumped through the system until a breakthrough curve was obtained in the UV-Vis spectrometer. The column was repacked with fresh silica each time a new asphaltene solution was pumped through the system. The back pressure regulator was pumped to 200 PSI and the flow rate used was 0.1 ml/min. The breakthrough curve was indicative of the adsorbed asphaltene.

Experiment I(B) – In this experiment the core holder was packed with HTAB pre-adsorbed silica particles. The remaining procedure was same as experiment I(A).

Experiment I(C) – In this experiment the core holder was packed with OTS functionalized silica particles. The remaining procedure was same as experiment I(A).

Experiment I(D) – In this experiment the core holder was packed HMDS functionalized silica particles. The remaining procedure was same as experiment I(A).

Experiment II(A) – In this experiment the core holder was packed with silica particles (oven heated at 150 °C for 24 hours to remove all the moisture from its surface) and the 0.5 wt.% polymer solution was pumped through the system for approximately 70 hours. The back pressure regulator was pumped to 200 PSI and the flow rate used was 0.1 ml/min. The adsorption of the polymer was measured by monitoring the pressure drop across the column. As the polymer adsorbed the pressure drop across the column increased which in turn was indicative of the decreasing porosity of the column. The porosity of the column was

calculated using the measured pressure drop in the Ergun equation as explained in the next section. As the polymer and the solvent had maximum absorbance in the same wavelength range, the absorbance of the effluent could not be tracked.

Experiment II(B) – In this experiment the core holder was packed with HTAB pre-adsorbed silica particles. The remaining procedure was same as experiment II(A).

2.6.Porosity, Ergun Equation and Adlayer Thickness Calculation

Porosity is the ratio of the volume of the pores to the bulk volume of the core holder. Ergun equation is used to measure the pressure drop across a packed column. It depends on the column length and porosity, properties of the fluid and the packing used.

$$\frac{\Delta P}{L} = 150 \left(\frac{\mu v_o}{D_p^2} \right) \frac{(1 - \varepsilon)^2}{\varepsilon^3} + \frac{7}{4} \left(\frac{\rho v_o^2}{D_p} \right) \frac{(1 - \varepsilon)}{\varepsilon}$$

Where,

ΔP = Differential pressure across the core holder

L = Length of the packing

μ = Viscosity of fluid

v_o = Superficial velocity of the fluid

D_p = Diameter of silica particles

ρ = Density of fluid

ε = Porosity

As the polymer adsorbs on to the silica particle surface, the differential pressure across the column increases. This value can be used to calculate the decreasing porosity of the column using the Ergun equation.

Adlayer thickness calculation using change in porosity:

Knowing all the parameters of the Ergun equation, the initial (ΔP_o) and the final (ΔP_{eq}) pressure drop across the column can be used to calculate the initial (ϵ_o) and the final (ϵ_{eq}) porosity of the column.

Volume of polymer adsorbed = $(\epsilon_o - \epsilon_{eq}) \times$ Bulk volume of column

Adlayer thickness = Volume of polymer / Area available for adsorption

Area available for adsorption was calculated assuming the silica particles to be spheres of diameter 100 μm .

Adlayer thickness calculation using the UV-Vis absorbance breakthrough curve:

The ratio of the area under the breakthrough curve to the total time of the experiment gave the concentration of the effluent. Knowing the mass of the effluent, concentration at the outlet was calculated. A mass balance of asphaltenes across the entire system further gave the weight of the asphaltenes adsorbed on the silica particles.

$(\text{Adsorbed})_{\text{asphaltene}} = (\text{mass IN})_{\text{asphaltene}} - (\text{mass OUT})_{\text{asphaltene}} - (\text{in system})_{\text{asphaltene}}$

Knowing the density of asphaltenes, the volume of adsorption was calculated. The ratio of volume of adsorption to the available surface area gave the adlayer thickness.

2.7. Sample Preparation for SEM Imaging

Three aluminum stubs were roughened using 320 grit sand paper followed by 600 grit sand paper. An extremely small quantity of the three asphaltene solutions were placed on the surface of the stubs using a dropper. The roughened surface helped increase the wettability of the stubs and spread the solution instantly. The stubs were dried in a vacuum oven at 200 °C overnight to evaporate the solvent. This left behind a very thin asphaltene layer that was used for imaging. A FEI-Sirion-XL30 scanning electron microscope was used to examine the specimens, which had been sputtered with a Gold-Palladium mixture approximately 10-nm thick. The accelerating voltage used was 5 keV, and a working distance of 5 mm was used for all measurements.

3. RESULTS AND DISCUSSION

3.1. Asphaltene Adsorption Studies

Our adsorption studies have been performed with three different concentrations of asphaltene solution. In the case of asphaltenes, the adsorbed amounts were used to develop Langmuir isotherms. The isotherms were plotted as amounts of asphaltene adsorbed (in mg) per unit area of silica versus the supernatant asphaltene concentration.

3.2. Shape of Isotherms

The amount of adsorbed asphaltenes per unit area of silica particles at various asphaltene concentrations was used to plot the linear Langmuir isotherm equation which is as follows:

$$\frac{1}{\Gamma} = \frac{1}{K C \Gamma_{max}} + \frac{1}{\Gamma_{max}}$$

where, Γ is the asphaltene adsorbed in mg/m^2 , C is the concentration of asphaltene solution in mg/lit , Γ_{max} is the saturation asphaltene adsorbed amount in mg/m^2 and K is the affinity constant in lit/mg . Using the intercept and slope obtained from the graph, Γ_{max} and K were calculated respectively. The saturation adsorption and affinity constant values thus obtained were used to plot the Langmuir isotherms whose equation is as follows:

$$\Gamma = \frac{K C \Gamma_{max}}{(1 + K C)}$$

Langmuir isotherm assumes the following:

- (a) the adsorption sites on the solid surface are equal in shape, size and have the same affinity for the adsorbate, i.e. the solid surface is homogenous
- (b) there are no solute-solute or solute-solvent interactions

(c) the adsorption is monolayer

Some of the above assumptions may not apply to the adsorption of asphaltenes. For example, it is well known that asphaltenes in any solution have a strong tendency to interact with each other through π – bonding and self-associate. Though, there have been a considerable number of studies where the Langmuir isotherm fit well to self-associating polymers and surfactants [23,24]. Both monolayer and multilayer adsorption isotherms have been discussed in previous studies. Though the monolayer, Langmuir adsorption isotherm is widely explored and published [13,25,26], several multilayer isotherm studies also exist [27,28,29]. The reason for this division is not clear though many believe that the type of adsorption largely depends on the source and aromaticity of asphaltenes [30].

The linear Langmuir equation fit well to all our studied systems with correlation coefficients ranging from 0.9437 to 1. Table 1 shows the amount of asphaltene adsorbed on pure and modified silica particles when different concentrations of dilute asphaltene solutions were pumped. 75.01 mg/m² of asphaltene was seen to adsorb on the pure silica column when 0.8 gm/lit of asphaltene solution was pumped through it. The adsorbed amount decreased for coated silica particles with HTAB pre-adsorbed silica adsorbing 64.9 mg/m², HMDS and OTS functionalized silica adsorbing 61.30 and 54.90 mg/m² respectively. HMDS functionalized silica adsorbed less than OTS functionalized silica for 0.8 and 1.6 gm/lit asphaltene solutions but adsorbed more when 3.2 gm/lit solution was pumped. HTAB pre-adsorbed silica always adsorbed asphaltenes less than pure silica but more than the silane functionalized silica particles.

Asphaltene Concentration	0.1 wt.% (0.8 gm/lit)		0.2 wt.% (1.6 gm/lit)		0.4 wt.% (3.2 gm/lit)	
Sample	Γ (mg/m ²)	nm	Γ (mg/m ²)	nm	Γ (mg/m ²)	nm
Pure Silica	75.01	62.74	141.33	117.78	253.44	211.20
HTAB	64.90	54.16	107.56	89.63	243.02	202.51
OTS	61.30	51.15	103.23	86.02	216.41	180.34
HMDS	54.90	45.75	84.36	70.30	219.24	182.7

Table 1: Amount of asphaltene adsorbed (mg/m²) and thickness of adsorption (assuming a density of 1.2 gm/cc) for three concentrations of asphaltenes on pure and modified silica particles.

Figure 5 (a), (b) and (c) show the SEM images of the 0.8, 1.6 and 3.2 gm/lit asphaltene aggregates. An area average diameter of these aggregates was calculated to be 62.22, 90.26 and 167.32 nm respectively. The diameters of the aggregates thus obtained fit in to the cluster region of the Yen-Mullins model [6]. The asphaltene cluster diameters were comparable to the thickness of the adlayers obtained for these concentrations, thus proving the assumption that the adsorptions were monolayer in nature. A good fit of the points to the linear Langmuir equation further confirms our assumption. The diameters obtained here were similar to previous studies that have examined asphaltenes by SEM and TEM. Pérez-Hernández et al. have reported diameters from ~ 350 to ~ 550 nm [31]. Unfortunately, elemental mapping of the aggregates was not possible due to a low resolution.

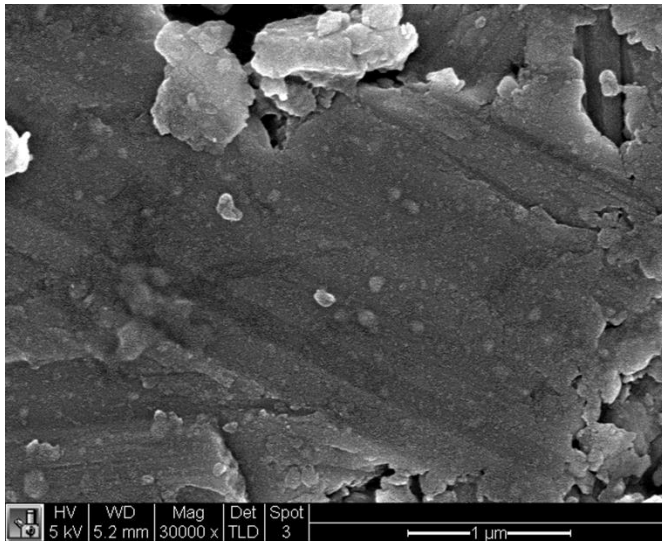


Fig.5(a)

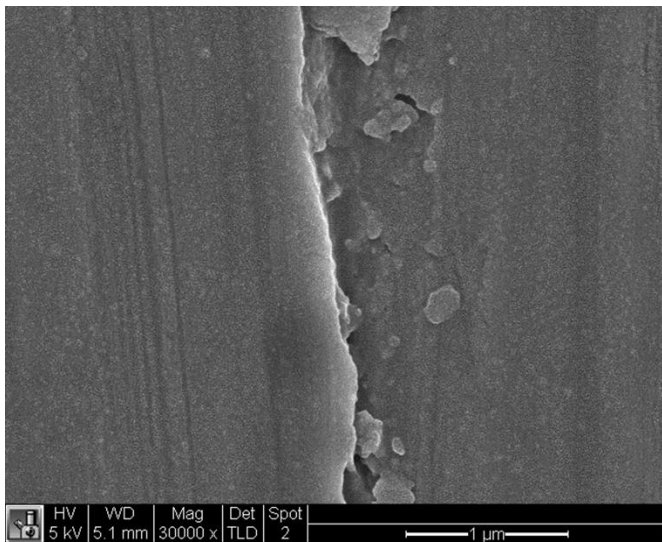


Fig.5(b)

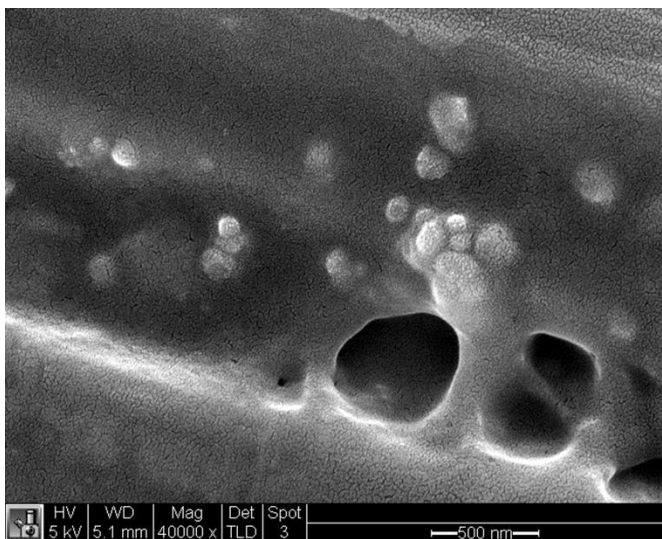


Fig. 5 (c)

Fig. 5: SEM images of the asphaltene aggregates (a) 0.1 wt.%, 0.8 gm/lit, (b) 0.2 wt.%, 1.6 gm/lit and (c) 0.4 wt.%, 3.2 gm/lit

Table 2 shows the correlation coefficients, saturation adsorption amount, affinity constant and the slopes and intercepts obtained for the linear Langmuir equation for the various silica columns. Figure 6 shows the isotherms that were developed using these values for all four types of silica. The highest asphaltene adsorption saturation was seen at 1250 gm/m² for pure silica. The modified silica particles showed reduced saturation adsorption, with HTAB coated silica at 909.10 gm/m², HMDS and OTS functionalized silica at 833.33 and 588.23 gm/m² respectively. As can be seen from fig. 6, saturation adsorption was projected to occur at high asphaltene concentrations (> 200 gm/lit) for all four cases. The thicknesses and saturation adsorption values in our experiments were much higher than the studies mentioned in the introduction. The most important difference between those studies and ours is the use of a very weak solvent that helped dissolve the asphaltene in its cluster form which is the reason for the same. Due to the lack of asphaltenes, experiments with solutions of high concentrations were not possible.

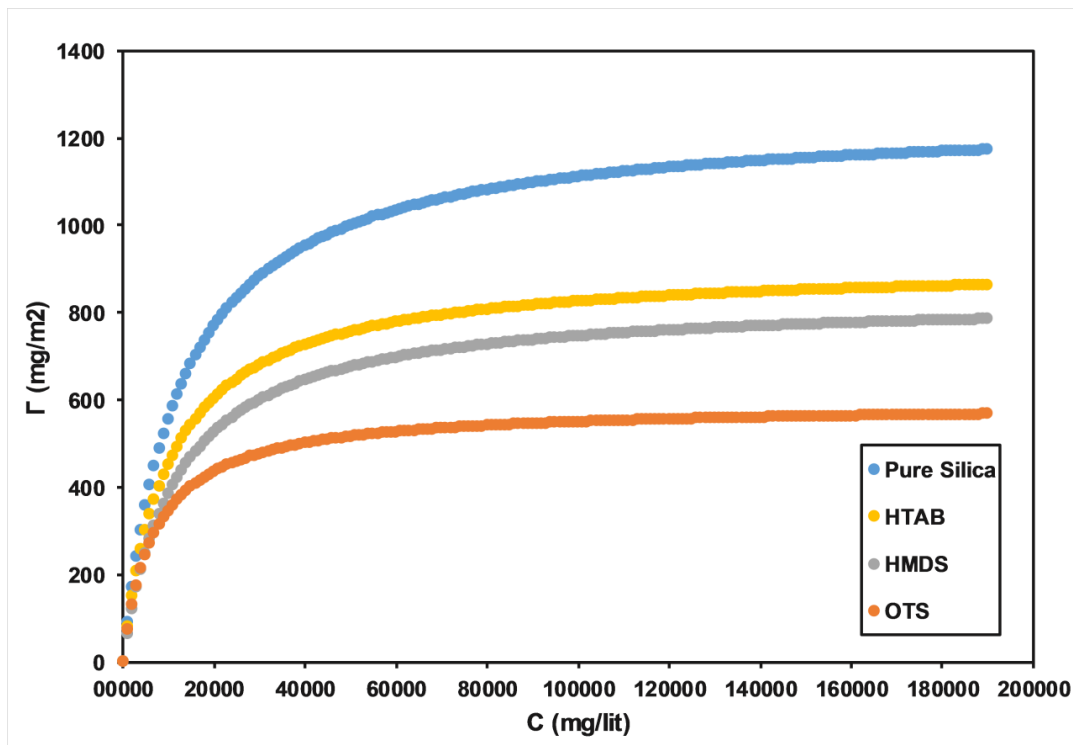


Fig 6: Langmuir isotherms for four types of silica pumped with asphaltene solutions at 22 °C

Silica Sample	Correlation Coefficient	Intercept $1/\Gamma_{\max}$ (m ² /mg)	Γ_{\max} (mg/m ²)	Slope	K (ml/mg)
Pure	1	0.0008	1250	10.011	0.079
HTAB pre-adsorbed	0.9798	0.0011	909.10	11.722	0.093
HMDS functionalized	0.9437	0.0012	833.33	14.065	0.085
OTS functionalized	0.9705	0.0017	588.23	11.941	0.142

Table 2: Correlation coefficients, slopes and intercepts obtained from the linear Langmuir equation; saturation adsorption of asphaltene and affinity constants for different silica samples.

Adsorption of an HTAB monomer gives the silanol groups a protection of 16 carbon atoms, while OTS provides an 18 carbon atom protection. Even though the two coatings have similar number of carbon atoms HTAB pre-adsorbed silica particles adsorbed asphaltenes much more than the OTS functionalized silica particles for all concentrations of asphaltene solutions. For that matter, they adsorbed more than the HMDS functionalized silica too. A reason for this maybe the adsorption of surfactant monomers being a weaker bond than the reacting silanes, the coating was not uniform throughout the particle. Surface defects could have exposed the underlying silanol groups and made the particles susceptible to asphaltene adsorption and deposition. As seen in the introduction, Turgman-Cohen et al., have successfully used silanes having 4 to 18 carbon atoms of chain lengths approximately 0.9-2.62 nm to reduce adsorption of asphaltene molecules of comparable sizes [14,15]. Our experiments have proven that the silanes are equally effective in reducing the adsorption of asphaltene aggregates having sizes about 60 times that of the silane alkyl chain. This is an important discovery as asphaltene aggregates of all sizes are encountered in the petroleum industry.

3.3.Polymer Adsorption Studies

The second part of the adsorption studies was to investigate the effect of multilayer adsorption on the porosity of the silica column. To effect this, an adsorption layer thick enough to considerably change the porosity was required. As the asphaltenes failed to produce large enough aggregates to accomplish the same, we shifted to a high molecular weight polymer. SEPTON 4099, a product of Kuraray Co. is patented as a thermoplastic polymer. Figure 7 shows a typical SEPTON molecule. The circle in fig. 7 represents an asphaltene molecule, it has a large aromatic core in the form of polystyrene rings surrounded by aliphatic chains, very similar to an asphaltene cluster. The polymer molecule as a whole represents an asphaltene cluster. A main difference between the polymer and asphaltenes is that the polymer lacks hetero atoms including metals.

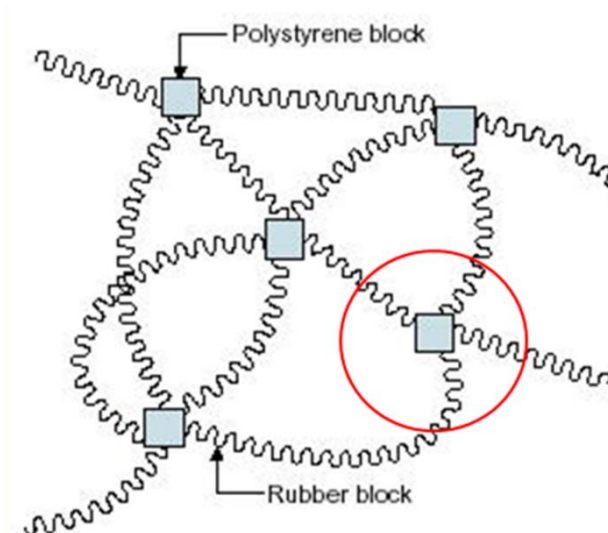


Fig 7: SEPTON 4099 molecule where the blue boxes represent a hard block (polystyrene) and the zig-zag line represent the soft block (hydrogenated polydiene). The red circle resembles an individual asphaltene molecule while the SEPTON molecule as a whole resembles an asphaltene cluster

Dilute solution of SEPTON 4099 was pumped through the column while closely monitoring the pressure drop (to maintain the same flow rate) using a Validyne DP 15 transducer. As the polymer and the solvent absorbed light in the same wavelength, UV-Vis absorbance could not be used in this case. The pressure drop across the column for pure solvent was recorded to be 0.15 PSI. This value was used to calculate the initial porosity (ϵ_0)

using the Ergun analysis and was found to be 0.38. Experiment II(A) – the polymer solution was kept pumping until a pressure breakthrough curve was obtained (approx. ~60 hours). The equilibrium pressure drop across the column was recorded as 0.93 PSI. Figure 8 shows the increase in pressure as the experiment progressed. Ergun analysis gave a value of 0.23 for the final porosity (ϵ_{eq}). Applying the Ergun analysis to every data point on fig. 8 showed how the porosity decreased with time. Figure 9 shows the change in porosity of the column over the course of 60 hours. Using the formulae and calculation methods mentioned in the previous section, an adlayer thickness of 3.67 microns was calculated. Figure 10 shows the buildup of the polymer adlayer calculated in the same manner. Though uniform adsorption throughout the column was assumed for the above calculations, an increase in pressure could also have been a result of plugging the front end of the column with the polymer. Proving our assumption right was important and to do so, micrographs of polymer adsorbed silica from the front and back end were taken. The polymer adsorbed silica was fairly sticky in nature and was spread between two glass slides to get a uniform layer for imaging. Figure 11(a) and 11(b) show the silica from the front and back ends respectively. It can be seen from the images that the polymer had adsorbed on both ends proving our assumption correct. Unfortunately, a direct measurement for the thickness of the adlayer could not be taken from these images.

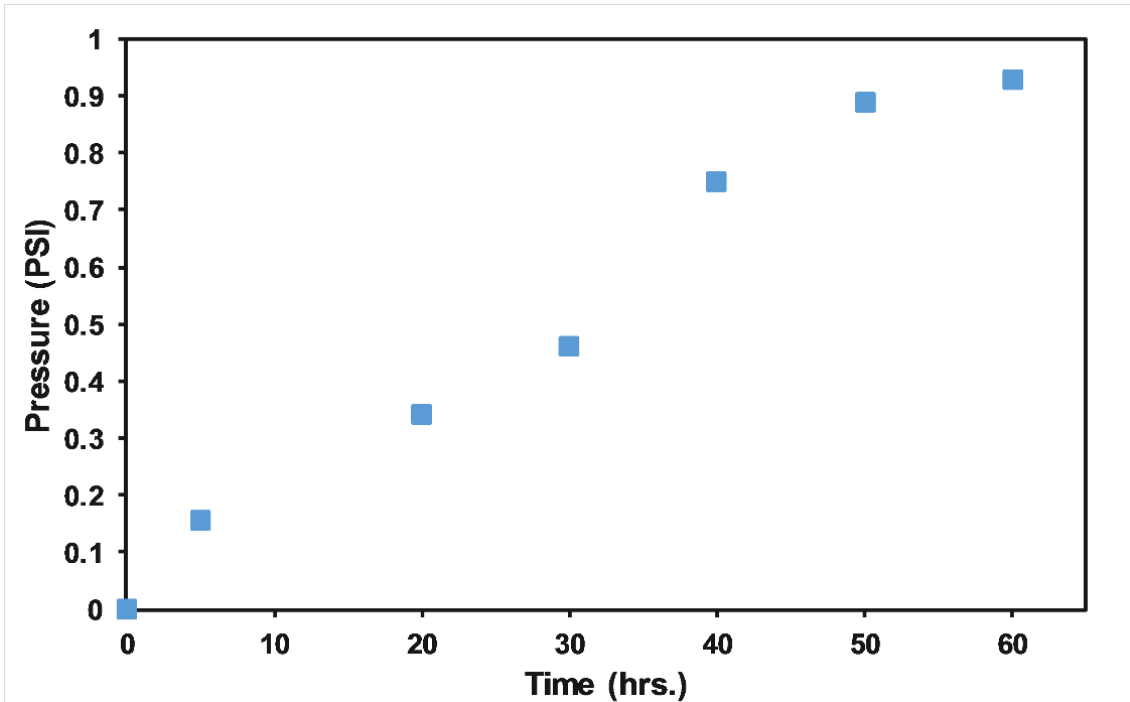


Fig 8: Increase in pressure drop across the silica column versus time as measured during experiment II (A)

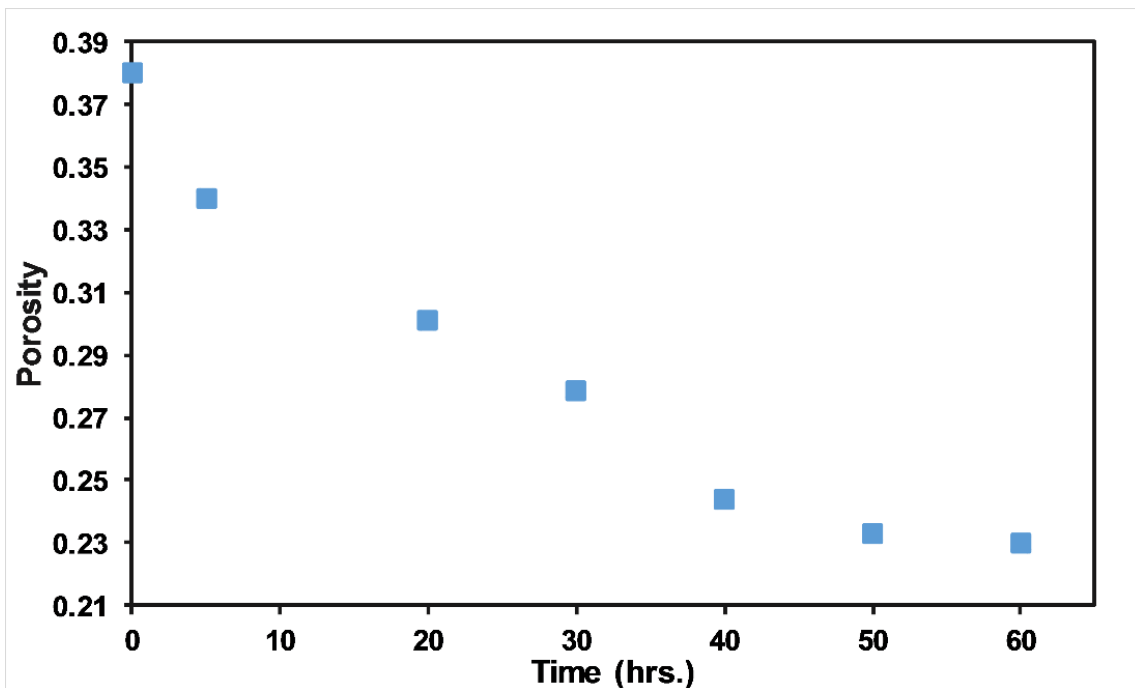


Fig 9: Decrease in porosity of the silica column versus time as calculated from Ergun analysis for experiment II (A)

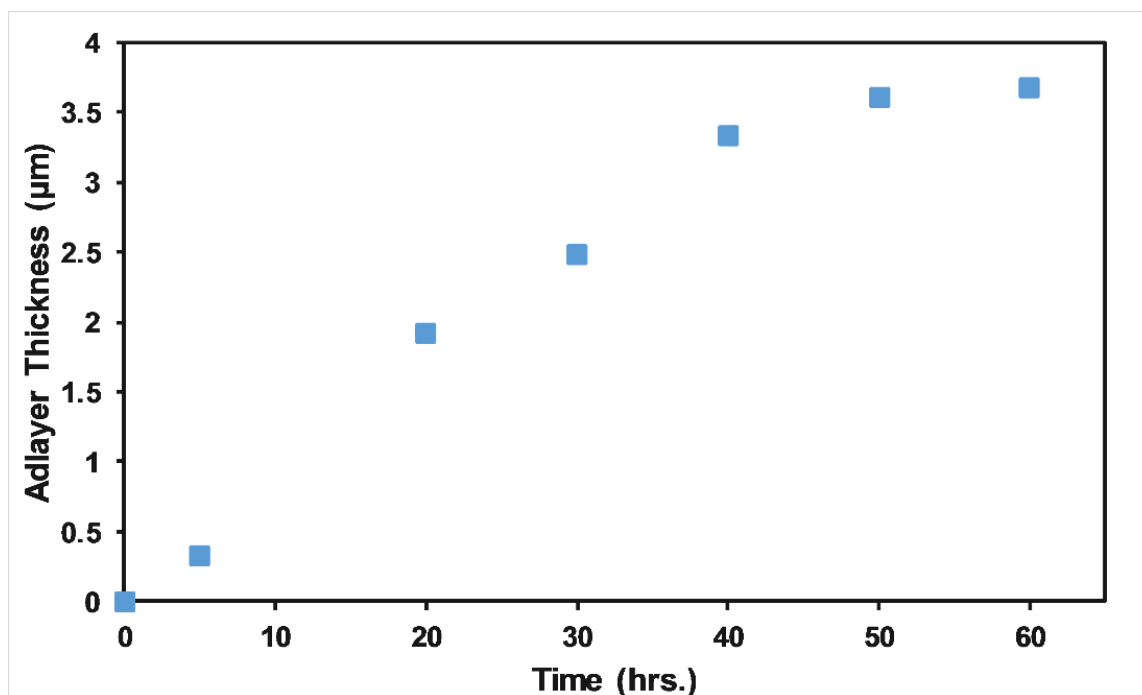


Fig 10: Development of the polymer adlayer as calculated for experiment II (A)

To prevent or reduce the adsorption of the polymer, silica was pre-adsorbed with HTAB using the procedure mentioned in the previous section. Experiment II(B) was also carried out for about 60 hours and no change in pressure drop was observed. Figure 12 shows the differential pressure reading across the column over the period of 60 hours. As there was no noticeable change in the pressure drop, Ergun analysis was not done. The pressure transducer has a company rating of ± 0.15 PSI. Owing to this noise, there were chances that a pressure increase below 0.15 PSI would not be detected. An increase in pressure of 0.15 PSI translates to an adlayer thickness of 1.85 microns, which is about 50% of the initial value (3.67 micron). Thus, it could be said that using a surfactant modification, the adlayer thickness was reduced to 50% of its initial value if not more. As a more accurate method could not be used to find the thickness of the adlayer, and as the first silica modification itself reduced the adlayer by 50%, further experiments with HMDS and OTS weren't performed. One reason why the adsorption of larger polymer aggregates was reduced to less than 50%

with the surfactant modification itself, maybe because the polymer lacked hetero atoms and metals in its structure making it less aromatic than the asphaltenes.

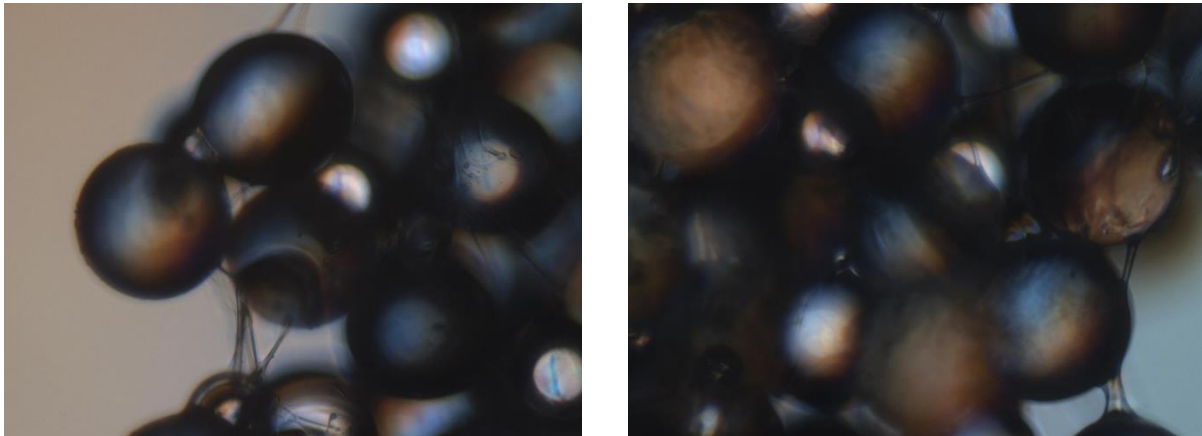


Fig 11: SEPTON adsorbed silica at (a) inlet of column and (b) out let of column

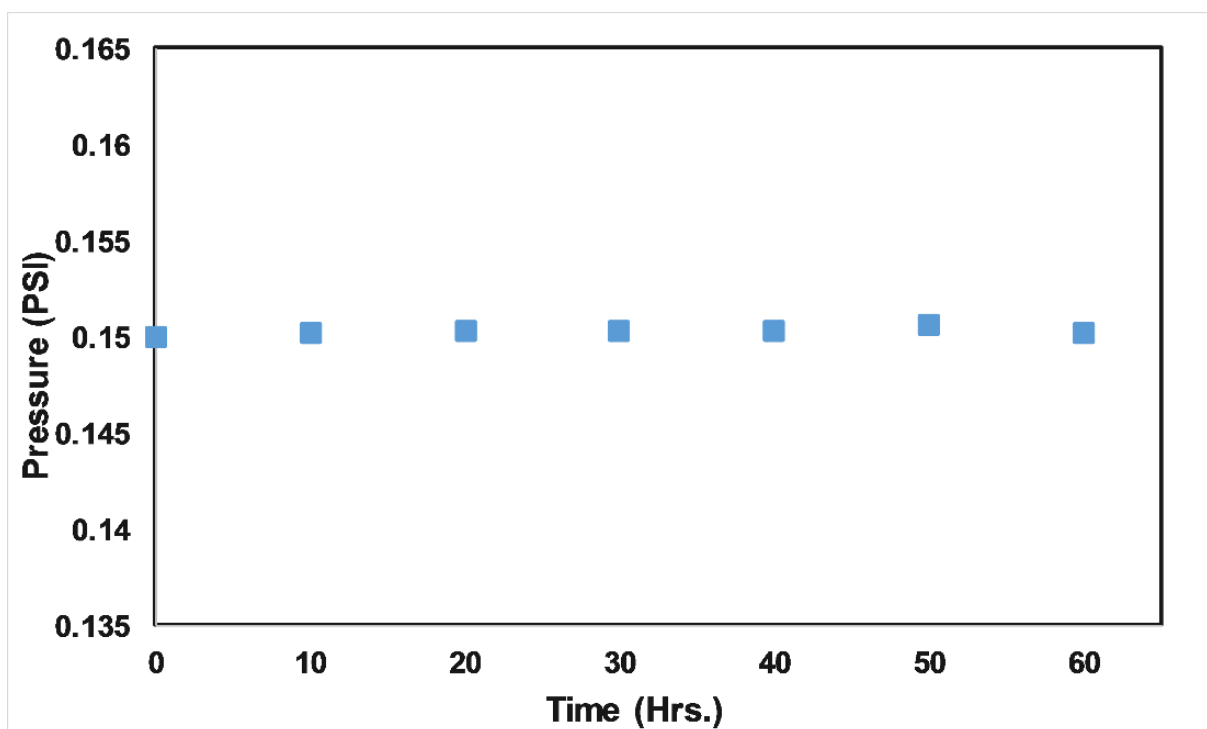


Fig 12: Pressure versus time graph as measured of experiment II (B)

4. CONCLUSION

By using a surfactant and a silane coating, the adsorption of asphaltene and polymer clusters were reduced to less than 50 % as compared to the adsorption on pure silica. Even though the HTAB (16 carbon atoms) and OTS (18 carbon atoms) hydrophobized the silica particles to a similar extent, HTAB pre-adsorbed silica adsorbed asphaltenes more than the silane functionalized silica owing to surface defects and a weak bonding. Thus reaffirming that, the hydrophobicity of the silanes has no role to play in the reduced adsorption but it is the property of the surfactant monomers and the silanes to protect the underlying silanol groups that helps reduce adsorption. The work also validates the effectiveness of silanes under flow conditions and at high pore pressures. Our studies also confirm that the silanes and for that matter even the HTAB monomer to a certain extent are effective in reducing the adsorption of asphaltene aggregates whose sizes are about 60 times that of the carbon tail. We believe that the findings in this research paper will be extremely useful while developing a protective coating for pipelines and other equipment in the upstream and downstream process involved in crude oil extraction.

5. REFERENCES

1. Groenzin, H.; Mullins, O. C., Asphaltene Molecular Size and Structure, *J. Phys. Chem. A* 1999, 103, 11237–11245.
2. Schuler, B; Meyer, G; Peña, D; Mullins, O. C; Gross, L., Unraveling the Molecular Structures of Asphaltenes by Atomic Force Microscopy, *J. Am. Chem. Soc.* 2015, 137, 9870–9876.
3. Sabbah, H.; Morrow, A. L.; Pomerantz, A. E.; Zare, R. N., Evidence for Island Structures as the Dominant Architecture of Asphaltenes, *Energy Fuels* 2011, 25, 1597–1604.
4. Karimi, A.; Qian, K.; Olmstead, W. N.; Freund, H.; Yung, C.; Gray, M. R., Quantitative evidence for bridged structures in asphaltenes by thin film pyrolysis, *Energy Fuels* 2011, 25, 3581–3589.
5. Borton, D.; Pinkston, D. S.; Hurt, M. R.; Tan, X.; Azyat, K.; Scherer, A.; Tykwinski, R.; Gray, M.; Qian, K.; Kenttämaa, H. I., *Energy Fuels* 2010, 24, 5548–5559.
6. Mullins, O. C., The Modified Yen Model, *Energy Fuels* 2010, 24, 2179–2207.
7. Mullins, O. C.; Sheu, E. Y.; Hammami, A.; Marshall, A. G. *Asphaltenes, Heavy Oils, and Petroleomics*; Springer: New York, 2007; Vol. 1.
8. Kazemzadeh, Y; Parsaei, R; Riazi, M., Experimental study of asphaltene precipitation prediction during gas injection to oil reservoirs by interfacial tension measurement, *Colloids and Surfaces A: Physicochemical and Engineering Aspects*, 2015, Vol.466, 138-146.
9. Akbarzadeh, K.; Hammami, A.; Kharrat, A.; Zhang, D.; Allenson, S.; Creek, J.; Kabir, S.; Jamaluddin, A.; Marshall, A. G.; Rodgers, R. P.; Mullins, O. C.; Solbakken, T. *Oilfield Rev.* 2007, 22–43.

10. Syunyaev, R. Z.; Balabin, R. M.; Akhatov, I. S.; Safieva, J. O., Adsorption of Petroleum Asphaltenes onto Reservoir Rock Sands Studied by Near-Infrared (NIR) Spectroscopy, *Energy Fuels* 2009, 23, 1230–1236.
11. Sheng, J., *Modern Chemical Enhanced Oil Recovery: Theory and Practice*; Gulf Professional Publishing: Burlington, MA, 2010.
12. Hannisdal, Andreas; Ese, Marit-Helen; Hemmingsen, Pål V.; Sjöblom, Johan, *Colloids and Surfaces A: Physicochemical and Engineering Aspects*, 2006, Vol. 276(1), 45-58.
13. Dudášová, Dorota; Simon, Sébastien; Hemmingsen, Pål V.; Sjöblom, Johan, *Colloids and Surfaces A: Physicochemical and Engineering Aspects*, 20 March 2008, Vol. 317(1-3), 1-9.
14. Turgman-Cohen, S.; Smith, M; Fischer, D; Kilpatrick, P; Genzer, J, Asphaltene Adsorption onto Self-Assembled Monolayers of Mixed Aromatic, *Langmuir*, 2009, Vol. 25(11).
15. Turgman-Cohen, S.; Fischer, D; Kilpatrick, P; Genzer, J, Asphaltene Adsorption onto Self-Assembled Monolayers of Alkyltrichlorosilanes of Varying Chain Length, *ACS Applied Materials & Interfaces*, 2009, Vol. 1(6).
16. Zahabi, A ; Gray, M. R. ; Dabros, T, Kinetics and properties of asphaltene adsorption on surfaces, *Energy and Fuels*, 2012, Vol. 26(2), 1009-1018.
17. Jouault, N.; Corvis, Y.; Cousin, F.; Jestin, J.; Barre, L., Asphaltene Adsorption Mechanisms on the Local Scale Probed by Neutron Reflectivity: Transition from Monolayer to Multilayer Growth above the Flocculation Threshold, *Langmuir* 2009, 25, 3991–3998.
18. Hamadou, R.; Khodja, M.; Kartout, M., Permeability Reduction by Asphaltenes and Resins Deposition in Porous Media, *Fuel* 2008, 87 (10–11), 2178–2185.

19. Moschopedis, S. E.; Fryer, J. F.; Speight, J. G., Quinone-type oxygen in petroleum asphaltenes and resins, *Fuel* 1976, 55, 227–232.
20. Spiecker, P. M.; Gawrys, K. L.; Kilpatrick, P. K., Aggregation and solubility behavior of asphaltenes and their subfractions, *J. Colloid Interface Sci.* 2003, 267, 178–193.
21. Jeramie J. A, Asphaltene Adsorption, a Literature Review, *Energy Fuels* 2014, 28, 2831–2856.
22. Gonzalez, V; Taylor, S. E., Asphaltene adsorption on quartz sand in the presence of pre-adsorbed water, *Journal of Colloid and Interface Science*, 15 October 2016, Vol.480, pp.137-145.
23. Simon, S; Picton, L; Le Cerf, D; Muller, G., Adsorption of amphiphilic polysaccharides onto polystyrene latex particles, *Polymer* 46 (2005), 3700–3707.
24. Aubry, T; Bossard, F; Moan, M., Laponite dispersions in the presence of an associative polymer, *Langmuir* 18 (2002) 155–159.
25. Saada, A; Siffert, B; Papirer, E., Comparison of the hydrophilicity/hydrophobicity of illites and kaolinites, *Journal of Colloid and Interface Science*, 1995, Vol. 174(1), 185-190.
26. Gaboriau, H; Saada, A., Influence of heavy organic pollutants of anthropic origin on PAH retention by kaolinite, *Chemosphere*, 2001, Vol. 44(7), 1633-1639.
27. Mendoza de La Cruz, José L. ; Castellanos-Ramírez, Iván V. ; Ortiz-Tapia, Arturo ; Buenrostro-González, Eduardo ; Durán-Valencia, Cecilia de Los A. ; López-Ramírez, Simón, Study of monolayer to multilayer adsorption of asphaltenes on reservoir rock minerals, *Colloids and Surfaces A: Physicochemical and Engineering Aspects*, 2009, Vol.340(1), 149-154.
28. Acevedo, S; Castillo, J; Fernández, A; Goncalves, S; Ranaudo, M. A., A study of multilayer adsorption of asphaltenes on glass surfaces by photothermal surface

- deformation. Relation of this adsorption to aggregate formation in solution, *Energy and Fuels*, 1998, Vol. 12(2), 386-390.
29. Jafari Behbahani, T; Ghotbi, C; Taghikhani, V; Shahrabadi, A., A new model based on multilayer kinetic adsorption mechanism for asphaltenes adsorption in porous media during dynamic condition, *Fluid Phase Equilibria*, 2014, Vol.375, 236-245.
30. Acevedo, S; Ranaudo, M. A.; Escobar, G; Gutiérrez, L; Ortega, P., Adsorption of asphaltenes and resins on organic and inorganic substrates and their correlation with precipitation problems in production well tubing, *Fuel*, 1995, Vol.74(4), 595-598.
31. Pérez-Hernández, R.; Mendoza-Anaya, D.; Mondragón-Galicia, G.; Espinosa, M. E.; Rodríguez-Lugo, V.; Lozada, M.; Arenas-Alatorre, Microstructural study of asphaltene precipitated with methylene chloride and n-hexane, *J. Fuel* 2003, 82, 977–982.